

DEVELOPMENT OF STREAMER SPARK CHAMBERS\*

F. Bulos, A. Boyarski, R. Diebold,  
B. Richter, A. Odian, F. Villa

Stanford Linear Accelerator Center  
Stanford University, Stanford, California

Recently, streamer spark chambers, or track chambers, have been described in the literature.<sup>1-10</sup> We have constructed such chambers, and describe some properties that have been observed. Such chambers are interesting in that tracks can be recorded for charged particles which pass in them in any arbitrary direction. In this sense the streamer chamber is similar to a bubble chamber, with the basic differences that it can be triggered on interesting events and the operating medium is a gas rather than a liquid.

Figure 1 shows the general test setup we have used in the studies. A ten stage Marx generator, capable of supplying up to a 250 kV pulse, drives one plate of a two electrode spark chamber. The sensitive volume of the chamber was 27 cm × 27 cm with a 12.5 cm gap. In order to allow photography through the plates, one of the electrodes was either conducting glass (Corning Glass Works) or a wire mesh made of 0.3 mm diameter wire strands spaced 6 mm apart. The chamber operated equally well for the two cases. A mirror was placed beside the chamber to allow photography of both the front view (along the E field) and the side view (perpendicular to the E field) on the same film. Counters placed above and below the chamber define the passage of charged particles through the chamber, and their coincidence pulses provide trigger pulses for the Marx generator. The minimum time delay between the passage of the particle and the application of the high voltage pulse on the chamber was 150 nsec.

---

\*Work supported by the U.S. Atomic Energy Commission.

(Paper presented at Purdue Conference on Instrumentation for High Energy Physics, Purdue University, Lafayette, Indiana, May 12-15, 1965)

A series gap and a shunt gap, each pressurized with nitrogen to 2 - 3 atmospheres, shape the pulse at the chamber. The series gap aids in producing a fast rise pulse while the shunt gap abruptly terminates the pulse at the chamber. Pulse widths at the chamber could be varied by adjusting the shunt gap separation or its pressure or both. Pulse rise times were typically 3 nsec, and the width could be made as short as 8 nsec at the base with a 200 kV amplitude.

Various gas mixtures were tried. From visual observation, neon or neon helium mixture (90% Ne - 10% He) provided tracks with the best definition. Other gases such as He, Ar, Ne plus few percent Ar, and Ne plus few percent Xe, gave somewhat poorer quality tracks. Pressures of 1 atmosphere were used. Cosmic rays or low energy  $\beta$  rays from a  $\text{Sr}^{90}$  source were used. In the latter case, one of the counters as well as two opposite sides of the chamber walls were made thin to allow for penetration by the  $\beta$  ray.

The theory of formation of the streamers is described in References 7,8,9. The free electrons left by the passing particle initiate avalanches along the E direction upon application of the high-voltage pulse. The avalanches then change into the streamer mode which results in rapid streamer buildup towards both electrodes of the chamber. Termination of the high-voltage pulse stops the streamer formation, leaving short localized streamers along the particle path.

The light output from the streamers decreases rapidly as the streamer length is shortened. In order to photograph streamers which are only a few millimeters long, it is necessary to use high speed film and large aperture lenses. Various high speed films have been tried. Best results have been obtained by the new Kodak film 2475 having an ASA rating of 1250. Tri-X also gave fairly good results, but its slower speed requires that the streamers be slightly longer. The streamer length is controlled by the high-voltage pulse amplitude and width. Short streamer lengths are generally the most luminous at the higher amplitudes and shorter pulse widths.

Tracks of high energy cosmic rays obtained with pulses of 200 kV amplitude and 12 nsec width at the base produced average streamer lengths of 3 to 4 mm as shown in Fig. 2. A 50 mm f/1.5 lens was used with the 2475 film. Since

there is a depth-of-field problem, the camera was focused midway between the front and side views, with a slight loss in definition in both views. The illustrated tracks show the track-following properties of this chamber. A low energy particle is seen to multiple scatter in the chamber. Also, many tracks can be supported simultaneously in this chamber; pictures have been taken with over 50 shower tracks in the chamber.

#### STREAMER SCATTER MEASUREMENTS

In order to determine the spacial accuracy with which tracks can be located, a study was made on the scatter of streamer dots from fitted trajectories for particles. Protons with 600 MeV/c momentum obtained from a target at the Stanford Mark III accelerator were made to pass parallel to the plates of the chamber. No magnetic field was used at the chamber. The delay time of the high-voltage pulse was about 0.3  $\mu$ sec after the passage of the particle. An 80 mm f/2.8 lens was used with a demagnification factor of 20 on the film. Tri-X film was used, and the average streamer lengths were about one centimeter. Track lengths were 24 cm at the chamber.

The coordinates (x,y) of each streamer in the front view (parallel to  $\vec{E}$ ) were measured and punched on cards. A least squares fit was then made to the points of each track having the form

$$y = a + bx + \frac{1}{2} c x^2$$

where a, b and c were varied. All tracks were oriented approximately along the x direction. From the distribution of the residuals

$$r_i = y_i - (a + b x_i + \frac{1}{2} c x_i^2)$$

the projected scatter of a streamer was determined to be 0.22 mm average for all the tracks.

A comparison can be made between the error in the curvature resulting from the streamer scatter and the actual curvature measurements "c" obtained from a large number of straight tracks. There were an average of 50 points per track, and if we approximate the streamer locations to one of uniform spacing along the track, we can use the curvature error estimates given by

Gluckstern.<sup>11</sup> For  $\sigma = 0.22$  mm, the curvature error due to statistical scatter is found to be  $1.4 \times 10^{-4}$  cm<sup>-1</sup>. The actual distribution in "c" from 44 tracks is shown in Fig. 3. The rms scatter is  $3.4 \times 10^{-4}$  cm<sup>-1</sup> which is considerably larger than the statistical error. Coulomb scattering in neon alone would give only  $0.6 \times 10^{-4}$  cm<sup>-1</sup> curvature error.

Using the measured curvature error of  $3.4 \times 10^{-4}$  cm<sup>-1</sup>, a chamber of 24 cm could observe momenta up to 10 BeV/c if a magnetic field of 10 kilogauss were used.

Similar streamer scatter measurements were also done on better quality tracks similar to those in Fig. 2. Cosmic rays with energy greater than 200 MeV were used. Scatter measurements were done for various delay times of the high-energy pulse applied to the chamber. The delays ranged from 150 nsec to 100  $\mu$ sec. The neon helium mixture was used in the chamber with no clearing field. Above 100  $\mu$ sec, the number of visible dots decrease with increasing delay time.

At short delay times, the streamers follow the particle trajectory, but after a few microseconds of delay the streamers diffuse about the trajectory as seen in Fig. 4. The projected scatter in the front view as a function of delay time is shown in Fig. 5. It is seen that the scatter varies as the square root of the delay time, as is expected from diffusion theory. The points fit the curve

$$\sigma^2 = 1640 \tau$$

where  $\sigma$  is the projected scatter in cm and  $\tau$  is in seconds.

Some quenching gases have been tried to reduce the 100  $\mu$ sec memory time of the chamber. Alcohol and SO<sub>2</sub> both have reduced the sensitive time to only a few microseconds, but the streamers also get fainter. Other quenching gases are being tried.

The distribution of scatter from the particle trajectory is shown in Fig. 6 at the 150 nsec delay. It agrees with a normal distribution with a 0.16 mm width. The scanning resolution, as determined by repeatedly measuring the coordinates of one dot, is only 0.05 mm. The streamer dot size in the front view was about 1.5 mm diameter.

In the side view, the streamers were about 4 mm long. A similar distribution gives a measuring error of 0.42 mm for streamer centers in this view.

We conclude that with a good optical system, streamers can be located to 0.16 mm in the front view and 0.42 mm in the side view.

#### GAP LENGTH DISTRIBUTION

The gap length distribution between adjacent streamers was measured at the shortest delay time. This is shown in Fig. 7. The expected distribution is exponential and the cut-off at about 2.0 mm indicates that approximately 50% of the streamers are prevented from developing by a robbing action between closely spaced streamers.

The exponential region for gap lengths greater than about 4 mm can be used to obtain the correct streamer density if robbing were not present. Thus we obtain the true mean gap as 2.77 mm and the mean streamer density as 3.6/cm. The number of streamers is a factor of 10 less than would be expected if each ion had a mean energy of about 35 eV given by the ionization potential.

Some measurements were made on particles with different ionizing power. Dot density measurements were made for minimum ionizing pions ( $I_{\min}$ ) and protons with  $2.3 I_{\min}$ . The ratio of the dot densities was found to be  $1.95 \pm 0.4$ , where the error is statistical over a 100 cm track length. The measured number is in agreement with the expected value 2.3 if the number of streamers were proportional to the ionizing power of the passing particle. The streamer chamber is thus capable of measuring  $dE/dx$  in this manner. However, it is very important that operating conditions remain constant during the recording.

The number of streamer dots at a delay of a few microseconds was found to be larger by about a factor of two over short delay times. This can be explained by the robbing action of closely adjacent streamers. At longer delay times the average separation between electrons is larger, so that the robbing is less and more streamers become visible.

## LIGHT AMPLIFICATION WITH AN IMAGE INTENSIFIER

A major drawback of the streamer chamber is the small amount of light that is available for photography. This means large aperture lenses are required with the resulting poor depth of field definition. An image intensifier can be used to both increase the amount of light and decrease the streamer length to obtain a chamber with true isotropic properties.<sup>12</sup>

A two stage tube made by RCA (C70012) having a 3-1/2-inch diameter photo-cathode and anode has been tried. The gain of such a tube is about 1500 and the resolution is better than about 25 lines/mm. Figure 8(a) shows a track taken with an f/5.6 aperture and longer streamer lengths (5 mm), while Fig. 8(b) shows short streamer lengths taken with an f/2.8 aperture. The latter tracks are essentially isotropic. In both cases, an f/2.8 coupling lens between the image tube anode and the film was used.

Isotropic tracks have been obtained with the f/2.8 objective lens. In order to photograph with an f/15 aperture, a higher gain intensifier is required. A three stage tube (RCA C70055) with a gain of about 50,000 will be tried in the near future.

The streamer chamber together with an image intensifier should be able to provide large volume three dimensional detectors. Plans are underway at SLAC to immerse such chambers in a magnetic volume of about 2 meters diameter and 1 meter depth. A larger Marx generator capable of providing a 600 kV pulse is being constructed for operation with larger chambers.

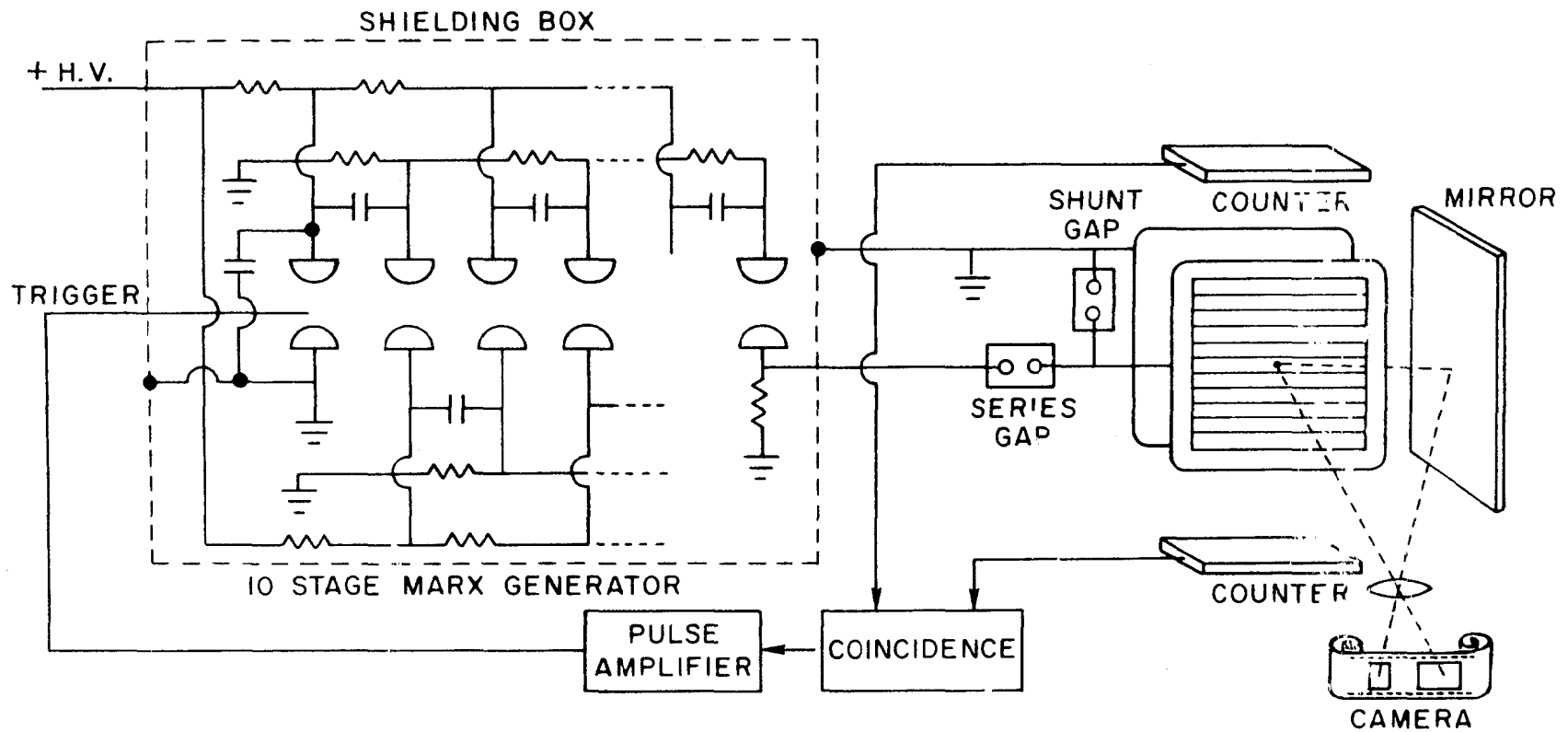


Fig.1--STREAMER CHAMBER APPARATUS

285-5-A

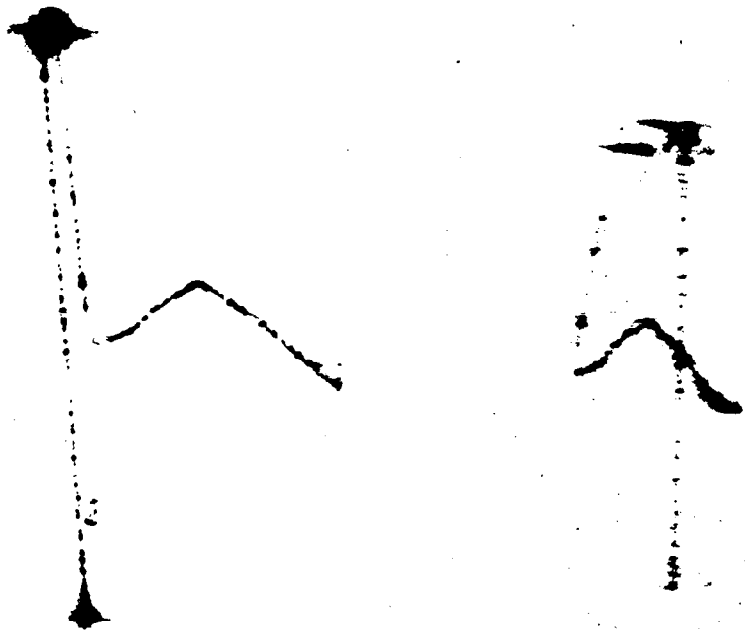


Fig. 2 (a)  $90^\circ$  stereo view of streamers, taken with F/1.5 lens aperture on 2475 film. Left side picture is view along E field. Streamers are 3-4 mm long. Chamber pulsed with 15 kv/cm and 12 nsec pulse width at base.

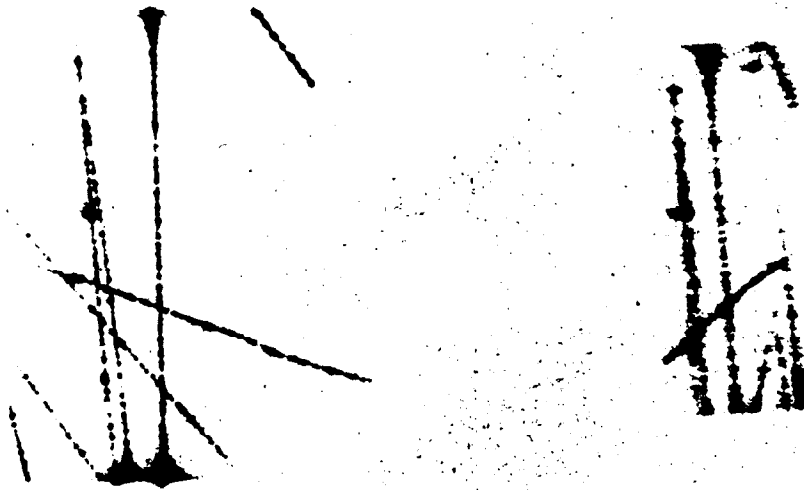


Fig. 2 (b)  $90^\circ$  stereo view, slightly longer streamers than in Fig. 1 (a).



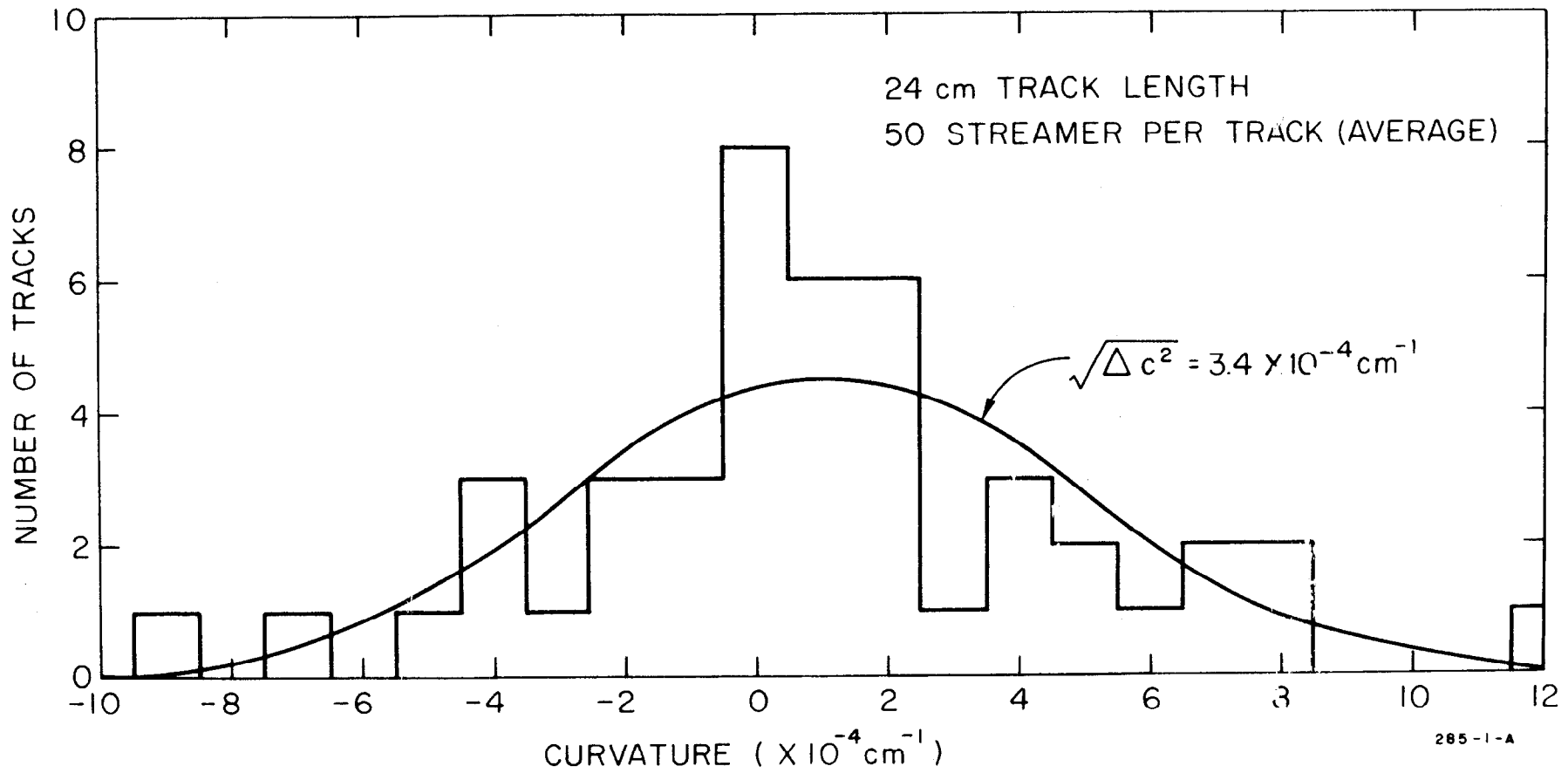


FIG. 3 - DISTRIBUTION OF CURVATURE MEASUREMENTS FOR DIFFERENT STRAIGHT TRACKS.

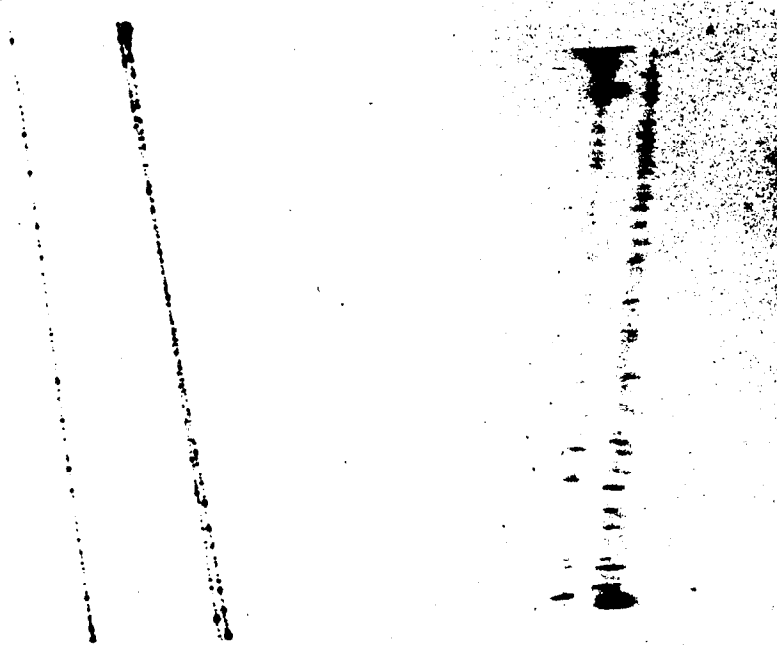


Fig. 4 (a) Streamer tracks for 0.15  $\mu$ sec delay in the h.v. pulse, photographed with F/2.8 lens aperture.

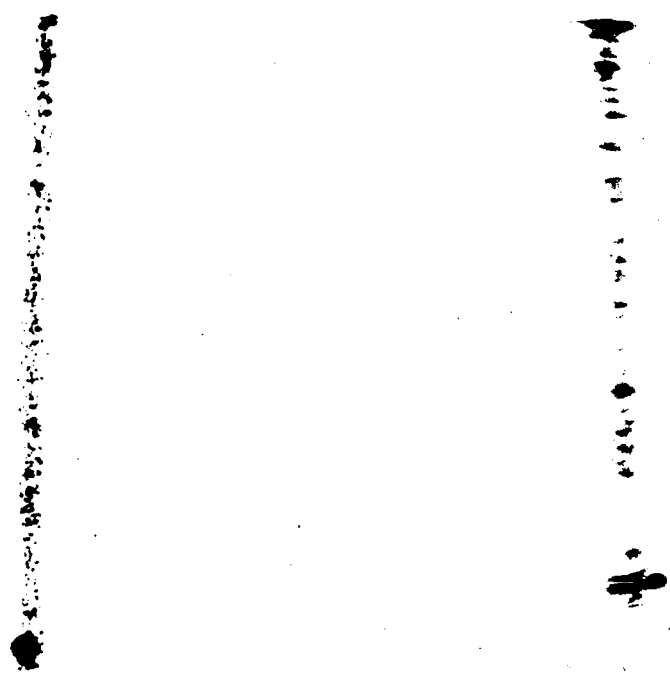


Fig. 4 (b) Streamer track as in Fig. 4 (a) but with a 20  $\mu$ sec delay in the h.v. pulse. Diffusion of the primary electrons is seen clearly in the view parallel to E (left side picture).

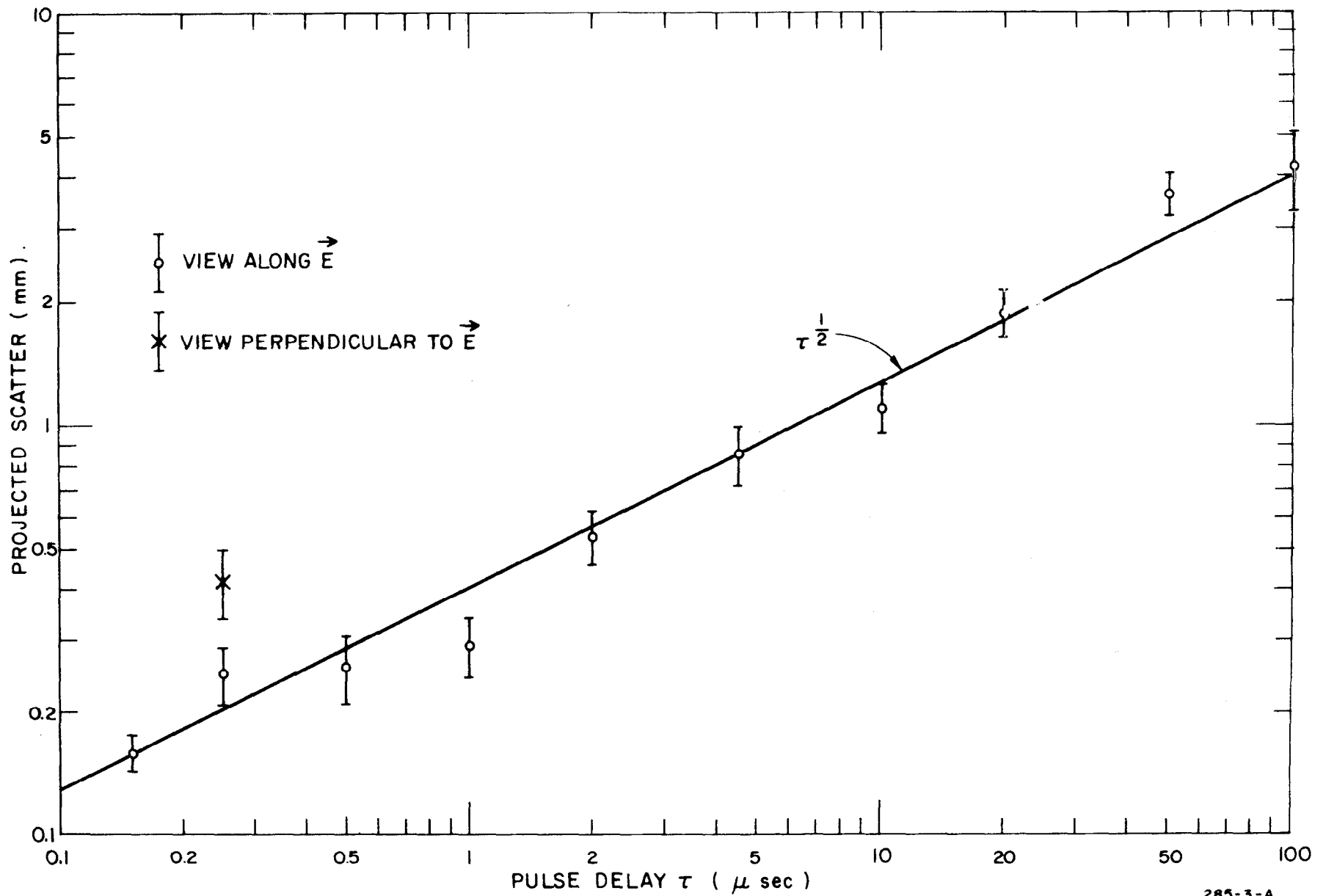
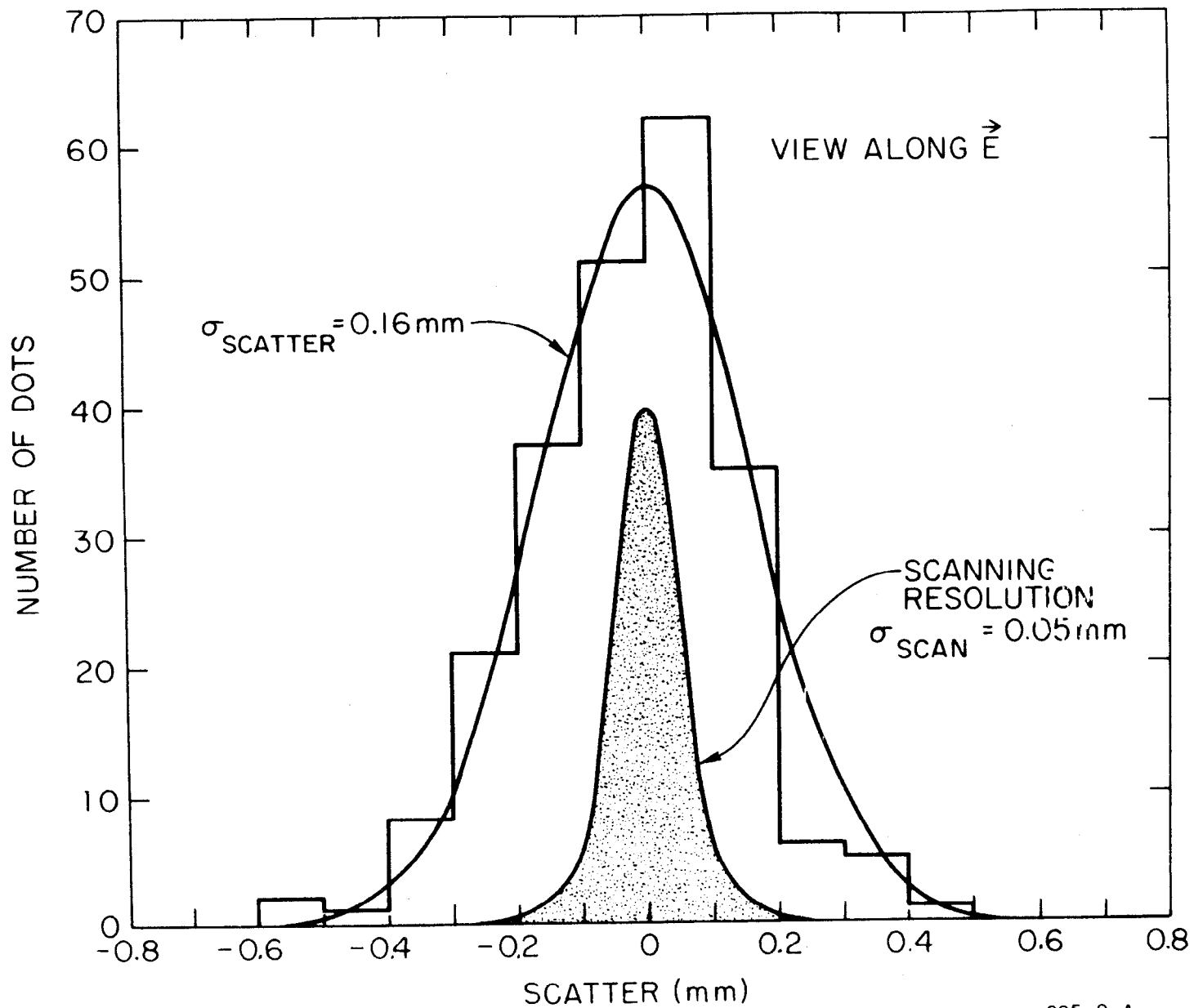


FIG. 5 -- PROJECTED SCATTER ( STANDARD DEVIATION ) OF STREAMERS FROM PARTICLE TRAJECTORY AS FUNCTION OF TIME DELAY OF HIGH VOLTAGE PULSE.



285-2-A

Fig. 6-SCATTERING DISTRIBUTION OF STREAMERS FROM PARTICLE TRAJECTORY WITH  $0.15 \mu\text{sec}$  H.V. PULSE DELAY

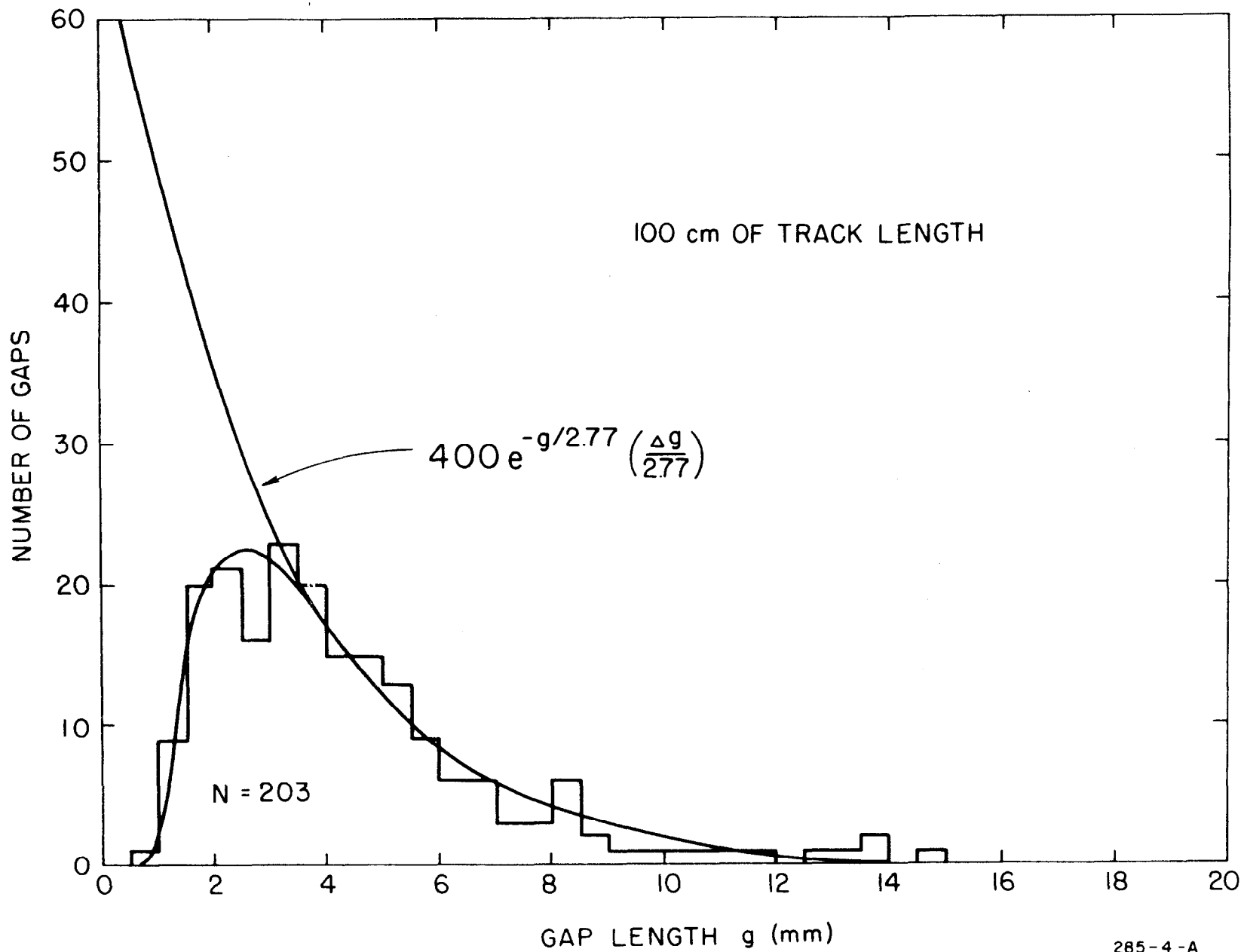


Fig. 7 -- STREAMER GAP LENGTH DISTRIBUTION FOR A 0.15  $\mu$ sec DELAYED H.V. PULSE

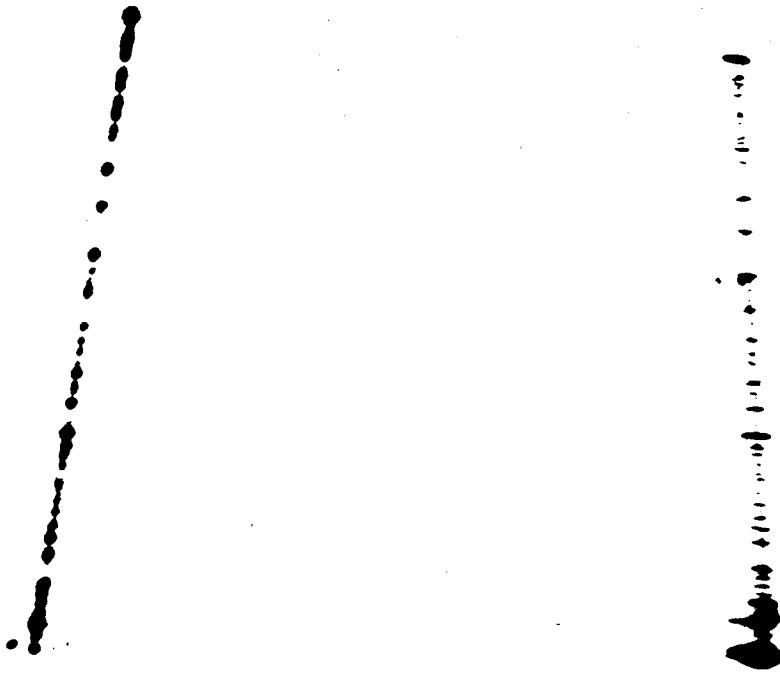


Fig. 8 (a) Stereo view of track viewed with a 2 stage intensifier. Front lens was 150 mm F/5.6, back lens between the anode and film was 80 mm F/2.8. Streamers are about 5 mm long.

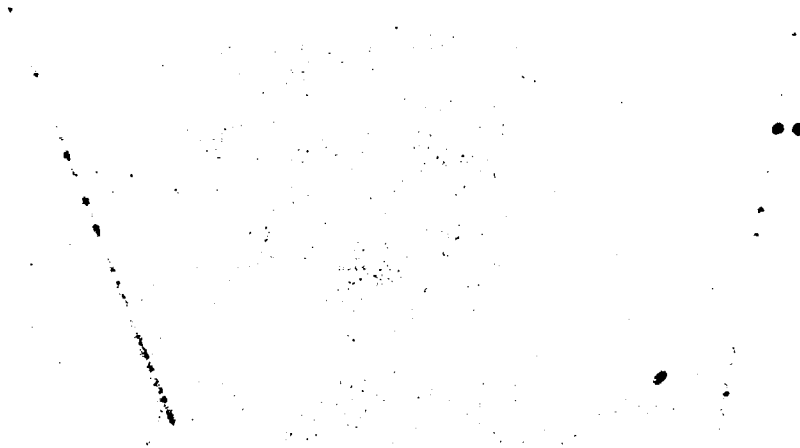


Fig. 8 (b) Stereo view as in Fig. 8 (a) but with shorter streamers. Front lens set at F/2.8. The tracks are essentially isotropic.

## REFERENCES

1. S. Fukui and S. Miyamoto, *Nuovo Cimento* 11, 113 (1959); *J. of the Phys. Soc. of Japan* 12, 2574 (1961).
2. A. A. Borisov, B. A. Dolgoshein, B. I. Luchkov, L. V. Reshetin and V. I. Ushakov, *Pribori i Tekhn. Exper.* 1, 49 (1962).
3. V. A. Mikhailov, V. N. Roinishvili and G. E. Chikovani, *Zh. Eksperim. i Teor. Fiz.* 45, 818 (1963); *JETP* 18, 561 (1964).
4. G. E. Chikovani, V. A. Mikhailov and V. N. Roinishvili, *Physics Letters* 6, 254 (1963).
5. A. I. Alikhanyan, T. L. Asatiani, E. M. Matevosyn, A. A. Nazaryan, and R. O. Sharkhatunyan, *Zh. Eksperim. i Teor. Fiz.* 45, 1684 (1963); *JETP* 18, 1154 (1964); *International Conference on Cosmic Rays*, Vol. 5, 540 Bombay (1964).
6. B. A. Dolgoshein and B. I. Luchkov, *Zh. Eksperim. i Teor. Fiz.* 46, 392 (1963); *JETP* 19, 266 (1964); *International Conference on Cosmic Rays*, Vol. 5, 530 Bombay (1964).
7. B. A. Dolgoshein, B. I. Luchkov and B. U. Rodionov, *Zh. Eksperim. i Teor. Fiz.* 46, 1953 (1963); *JETP* 19, 1315 (1964).
8. G. E. Chikovani, V. N. Roinishvili and V. A. Mikhailov, *Zh. Eksperim. i Teor. Fiz.* 46, 1228 (1964); *JETP* 19, 833 (1964); *International Conference on Cosmic Rays* Vol. 5, 517 Bombay (1964).
9. E. Gygi and F. Schneider, *CERN* 64-30 (351); *CERN* 63-37 (145).
10. I. V. Falomkin, M. M. Kulyukin, D. B. Pontecorvo, Yu. A. Sherbakov, *Nuovo Cimento* (10), 34, 1394 (1964).
11. R. L. Gluckstern, *Nucl. Instr. and Methods* 24, 381 (1963).
12. M. M. But-slov, V. I. Komarov and O. V. Sarchenko, *Zh. Eksperim. i Teor. Fiz.* 46, 2245, (1964); *JETP* 19, 1516 (1964).